N° d'ordre :
N° de série :

KASDI MERBAH UNIVERSITY OUARGLA

Faculty of Mathematics and Material Sciences

Department of Mathematics

Path: Mathematics
Specialization: Functional Analysis

A Thesis Submitted to Obtain the Degree of

MASTER

Theme:

Inverse Problem For Some Fractional Differential Equations

By:

Saada Nadira

Defended on: 04/06/2026

Jury Members:

Mr.	**Bensayah Abdallah**	Prof. Kasdi Merbah University-Ouargla	Chairman
Mr.	**Merabet Ismail**	Prof. Kasdi Merbah University-Ouargla	Examiner
Ms.	**Messaoudi Djemaa**	M.C.A. Kasdi Merbah University-Ouargla	Supervisor

Dedication

Praise be to Allah, *who has granted me time and illuminated my path to appreciate this step in my academic journey. I entrust success and guidance to Him, and I seek His support in completing this work, the fruit of effort and achievement, by His grace.*

To the One who gave me life, hope, and an upbringing filled with a passion for learning and knowledge, To my dear parents, may Allah protect and preserve them, and to my entire family and my friends, and to my fellow students. May God grant them success.

I dedicate this humble work to every teacher who has enriched us with the knowledge and wisdom granted by Allah, from the earliest stages of my education until this moment.

ACKNOWLEDGEMENT

First and foremost, all praise and gratitude are due to Allah, who granted me the strength, patience, and determination to complete this work and overcome the challenges encountered throughout my academic journey. I would like to express my sincere gratitude and deepest appreciation to my supervisor, **Dr. Messaoudi Djemaa** for her invaluable guidance, insightful advice, continuous support, and constructive remarks throughout the preparation of this dissertation. Her encouragement and dedication have greatly contributed to the successful completion of this work. It is a great honor for me to extend to her my highest respect and appreciation. My sincere thanks also go to all the professors of the Department of Mathematics for their dedication, support, and the knowledge they generously shared throughout my years of study. Finally, I would like to thank everyone who contributed, directly or indirectly, to the completion of this work. May Allah reward them all and grant them continued success in their academic and professional endeavors.

"All praise and gratitude be to Allah, who granted me patience to overcome the

difficulties I faced in completing this humble work.

Contents

Notations

- $\partial_t u$: Partial derivative of u with respect to time t.
- ∇: Gradient operator.
- Δ: Laplacian operator.
- $\partial_t^\alpha u$: Caputo fractional derivative of order $\alpha \in (0,1)$.
- $L^p(\Omega)$: Lebesgue space of p-integrable functions on Ω,
  $L^p(\Omega) = \{v : \Omega \to \mathbb{R} \text{ measurable}; \|v\|_p < \infty\}$.
- $L^\infty(\Omega)$: Space of essentially bounded functions on Ω.
- $L^2(\Omega)$: Hilbert space of square-integrable functions on Ω, with:

$$\|v\|_{L^2(\Omega)} = \left(\int_\Omega |v(x)|^2 \, dx \right)^{1/2}.$$

- $H^k(\Omega)$ or $W^{k,p}(\Omega)$: Sobolev spaces with weak derivatives up to order k in L^p.
- $H^1(\Omega)$: Sobolev space,
  $H^1(\Omega) = \left\{ v \in L^2(\Omega) : \nabla v \in (L^2(\Omega))^d \right\}$.
- $\|v\|_{1,\Omega} = \left(\|v\|^2_{L^2(\Omega)} + \|\nabla v\|^2_{L^2(\Omega)} \right)^{1/2}$.

- $H_0^1(\Omega)$: Functions in $H^1(\Omega)$ with zero trace on the boundary:
  $H_0^1(\Omega) = \{v \in H^1(\Omega) : v|_{\partial\Omega} = 0\}$.
- $H^{-1}(\Omega)$: The dual space of $H_0^1(\Omega)$.
- L^m: Hilbert space, with $m \in \mathbb{R}$.
- H^m: Sobolev space, with $m \in \mathbb{R}$.
- $\|u\|_{H^m(0,T;B)} = \left(\sum_{k=0}^{m} \int_0^T \|u^{(k)}(t)\|_B^2 \, dt\right)^{1/2}$.
- $H^m(0,T;B) = \left\{u(t) \in B \text{ for a.e. } t \in (0,T) \text{ and } \|u\|_{H^m(0,T;B)} < \infty\right\}$.
- $\rightharpoonup$: Weak convergence.
- $\rightarrow$: Strong convergence.

Introduction

Inverse problems constitute an important branch of applied mathematics whose objective is to determine unknown parameters, coefficients, sources, or system characteristics from indirect observations. In contrast to direct problems, where the governing parameters are known and the corresponding system response is computed, inverse problems seek to recover hidden information from measured data. Such problems arise naturally in many scientific and engineering applications where direct measurements are difficult, expensive, or impossible to obtain.

The mathematical study of inverse problems has experienced remarkable development during the last decades due to its numerous applications in science and technology. Fundamental contributions have established the theoretical framework for the analysis of inverse problems and their inherent difficulties related to existence, uniqueness, and stability of solutions [6]. In many practical situations, inverse problems are ill-posed in the sense of Hadamard, meaning that small perturbations in the measurement data may produce large variations in the reconstructed quantities. Consequently, the design of stable reconstruction procedures has become a central topic in inverse problem theory.

Among the various classes of inverse problems, coefficient identification problems have attracted considerable attention because of their importance in heat transfer, fluid dynamics, geophysics, environmental sciences, and material characterization. Numerous theoretical and numerical methods have been developed for the recovery of unknown coefficients appearing in partial differential equations. Recent contributions include optimization-based approaches, regularized iterative methods, and parameter estimation techniques for nonlinear inverse problems [1, 17, 18, 19, 20]. These works demonstrate the effectiveness of modern regularization and optimization strategies for recovering unknown physical parameters from incomplete and noisy observations.

Fractional calculus has emerged as a powerful mathematical framework for describing physical processes involving memory effects and nonlocal interactions. Unlike classical differential equations, fractional models incorporate hereditary properties that allow a more realistic representation of many complex phenomena. Fractional differential equations have proved particularly successful in the modeling of anomalous diffusion processes encountered in porous media, biological tissues, viscoelastic materials, and heterogeneous environments [22]. Their ability to capture long-range temporal memory and nonlocal dynamics has motivated extensive theoretical and numerical investigations.

In recent years, increasing attention has been devoted to inverse problems associated with fractional diffusion equations. Significant progress has been achieved concerning uniqueness, stability, and numerical reconstruction of unknown coefficients and model parameters. Notable contributions include uniqueness results for fractional diffusion equations [3, 13], reconstruction of diffusion coefficients in subdiffusion models [12, 15], simultaneous recovery of diffusion coefficients and fractional orders [16], as well as the identification of unknown coefficients and potentials in fractional diffusion equations [25, 26]. These studies highlight both the practical importance and the mathematical challenges associated with inverse fractional diffusion problems.

Many real-world diffusion processes take place in heterogeneous media whose properties vary spatially throughout the domain. To model such situations more accurately, variable-order fractional diffusion equations have been introduced. In these models, the diffusion dynamics are influenced not only by the diffusion coefficient but also by a spatially dependent fractional structure that reflects the heterogeneity of the medium. Such equations provide a flexible framework for describing complex transport phenomena and have motivated substantial research efforts concerning their analysis and numerical approximation [13].

Despite these advances, inverse coefficient problems for variable-order fractional diffusion equations remain challenging due to the combined effects of nonlocality, heterogeneity, and ill-posedness. The recovery of unknown diffusion coefficients from indirect measurements requires the development of robust mathematical formulations together with efficient computational algorithms capable of producing stable reconstructions in the presence of noise.

The present thesis is devoted to the study of an inverse coefficient problem associated in a time-fractional diffusion equation. The objective is to reconstruct an unknown spatially varying diffusion coefficient from observations of the state variable. To overcome the ill-posedness of the problem, a Tikhonov regularization framework is employed. The theoretical analysis focuses on the properties of the parameter-to-state map, the existence of regularized solutions, and the stability and convergence of the proposed formulation.

For the numerical approximation, the forward problem is discretized using the finite element method in space and convolution quadrature in time. The resulting finite-dimensional optimization problem is solved using the Nelder–Mead simplex method [21], implemented through the SciPy scientific computing library [24]. The proposed methodology provides stable numerical reconstructions from noisy observations and enables the investigation of the influence of regularization and measurement errors on the quality of the recovered coefficients.

The thesis is organized as follows.

- **Chapter 1** presents the mathematical background required for the study of the proposed inverse problem. Fundamental concepts of inverse problems, fractional calculus, and fractional diffusion equations are introduced, and the forward and inverse problems are formulated.

- **Chapter 2** is devoted to the theoretical analysis of the inverse coefficient problem. The parameter-to-state map is investigated, the ill-posedness of the reconstruction problem is discussed, and a Tikhonov regularization framework is established. Existence, stability, convergence, and identifiability results are proved.

- **Chapter 3** develops the numerical approximation and reconstruction methodology. The finite element discretization of the spatial variables and the convolution quadrature approximation of the fractional derivative are presented. The discrete inverse problem is formulated and solved using the Nelder–Mead optimization algorithm.

- **Chapter 4** presents numerical experiments illustrating the effectiveness of the proposed reconstruction method. Synthetic observation data are employed to evaluate the accuracy, stability, and robustness of the numerical procedure under different reconstruction scenarios and noise levels.

Chapter 1

Forward problem for fractional differential equations

1.1 Fractional calculus background

Fractional calculus is a natural extension of classical calculus in which the orders of differentiation and integration are allowed to take arbitrary real or even complex values and has been extensively studied in the literature [2, 14, 22]. Although the idea of non-integer order differentiation can be traced back to a correspondence between Leibniz and L'Hôpital in 1695, the rigorous mathematical foundations of fractional calculus were established much later through the works of Liouville, Riemann, Grünwald, Letnikov, and Caputo.

In recent decades, fractional differential equations have attracted considerable attention due to their ability to model memory and hereditary effects that cannot be adequately described by classical integer-order models. Applications arise in anomalous diffusion, viscoelasticity, porous media, biology, finance, control theory, and many other fields. In particular, time-fractional diffusion equations provide an effective framework for describing subdiffusive transport processes, where the mean square displacement grows slower than linearly with time.

The mathematical formulation of fractional differential equations relies on several fractional operators. We begin by introducing the Gamma function, which plays a fundamental role in the definition of fractional integrals and derivatives.

1.1.1 The Gamma function

The Gamma function appears naturally in the definition of fractional integrals and derivatives and plays a central role in the analysis of time-fractional diffusion equations.

Definition 1.1.1 (Gamma function) *For every real number $z > 0$, the Gamma function is defined by*

$$\Gamma(z) = \int_0^\infty t^{z-1} e^{-t} \, dt.$$

A fundamental property of the Gamma function is the recurrence relation

$$\Gamma(z+1) = z\,\Gamma(z),$$

which immediately yields

$$\Gamma(n) = (n-1)!, \qquad n \in \mathbb{N}.$$

Consequently, the Gamma function generalizes the factorial function while preserving its most important algebraic properties.

1.1.2 Riemann-Liouville fractional integrals

Fractional integration constitutes the foundation of fractional calculus. The most widely used definition is the Riemann-Liouville fractional integral.

Definition 1.1.2 (Left-sided Riemann–Liouville fractional integral) *Let $f \in L^1(a, b)$ and let $\alpha > 0$. The left-sided Riemann–Liouville fractional integral of order α is defined by*

$$(I_{a+}^{\alpha} f)(t) = \frac{1}{\Gamma(\alpha)} \int_a^t (t-\tau)^{\alpha-1} f(\tau)\, d\tau, \qquad t > a.$$

Similarly, the right-sided fractional integral is defined as follows.

Definition 1.1.3 (Right-sided Riemann–Liouville fractional integral) *Let $f \in L^1(a,b)$ and let $\alpha > 0$. The right-sided Riemann–Liouville fractional integral of order α is given by*

$$(I_{b-}^{\alpha} f)(t) = \frac{1}{\Gamma(\alpha)} \int_t^b (\tau - t)^{\alpha-1} f(\tau)\, d\tau, \qquad t < b.$$

When $\alpha = 1$, the fractional integral reduces to the classical integral operator. Indeed,

$$(I_{a+}^{1} f)(t) = \int_a^t f(\tau)\, d\tau.$$

Therefore, the Riemann–Liouville operator can be viewed as a natural extension of ordinary integration to arbitrary positive orders.

1.1.3 Fundamental properties of fractional integrals

The Riemann–Liouville fractional integral satisfies several properties that closely resemble those of classical integration.

Theorem 1.1.4 (Linearity) *[14, 22] Let f and g be integrable functions and let $c_1, c_2 \in \mathbb{R}$. Then*

$$I_{a+}^{\alpha} (c_1 f + c_2 g) = c_1 I_{a+}^{\alpha} f + c_2 I_{a+}^{\alpha} g.$$

Similarly,

$$I_{b-}^{\alpha} (c_1 f + c_2 g) = c_1 I_{b-}^{\alpha} f + c_2 I_{b-}^{\alpha} g.$$

The next property is one of the cornerstones of fractional calculus.

Theorem 1.1.5 (Semigroup property) *[14, 22] For every $\alpha, \beta > 0$, the left-sided fractional integrals satisfy*

$$I_{a+}^{\alpha} I_{a+}^{\beta} = I_{a+}^{\alpha+\beta}.$$

Likewise, the right-sided fractional integrals satisfy

$$I_{b-}^{\alpha} I_{b-}^{\beta} = I_{b-}^{\alpha+\beta}.$$

The semigroup property shows that successive applications of fractional integrals combine in exactly the same way as repeated applications of classical integration. This property plays a fundamental role in the construction of fractional differential operators and in the analysis of fractional evolution equations.

1.1.4 Caputo fractional derivative

Although several definitions of fractional derivatives exist, the Caputo derivative is particularly suitable for physical applications because it allows the use of classical initial conditions.

Definition 1.1.6 (Caputo fractional derivative) *Let $n - 1 < \alpha < n$, where $n \in \mathbb{N}$. The left-sided Caputo fractional derivative of order α is defined by*

$${}^{C}D_{a+}^{\alpha} f(t) = \frac{1}{\Gamma(n-\alpha)} \int_a^t (t-\tau)^{n-\alpha-1} f^{(n)}(\tau)\, d\tau.$$

For the diffusion problems considered in this thesis, the fractional order satisfies $0 < \alpha < 1$. In this case, the Caputo derivative takes the simpler form

$${}^{C}D_{a+}^{\alpha} f(t) = \frac{1}{\Gamma(1-\alpha)} \int_a^t (t-\tau)^{-\alpha} f'(\tau)\, d\tau.$$

The Caputo derivative incorporates the entire history of the function through the convolution kernel $(t-\tau)^{-\alpha}$, which explains the memory effect characteristic of fractional differential equations.

1.1.5 Basic properties of the Caputo fractional derivative

The Caputo fractional derivative possesses several important properties that make it particularly attractive for modeling physical phenomena. Unlike the Riemann–Liouville derivative, the Caputo derivative preserves the classical interpretation of initial conditions and naturally incorporates memory effects.

The following results will be used repeatedly throughout the thesis.

Proposition 1.1.7 (Linearity) *Let f and g be sufficiently smooth functions and let $c_1, c_2 \in \mathbb{R}$. Then*

$$ {}^{C}D^{\alpha}_{a+}\left(c_1 f + c_2 g\right) = c_1\, {}^{C}D^{\alpha}_{a+} f + c_2\, {}^{C}D^{\alpha}_{a+} g. $$

Therefore, the Caputo derivative is a linear operator.

Proposition 1.1.8 (Derivative of a constant) *Let C be a constant. Then*

$$ {}^{C}D^{\alpha}_{a+} C = 0. $$

This property is one of the principal reasons why the Caputo derivative is preferred in many applications. In contrast, the Riemann–Liouville derivative of a constant is generally nonzero.

Proposition 1.1.9 (Fractional integration formula) *Let $n-1 < \alpha < n$. Then*

$$ I^{\alpha}_{a+}\left({}^{C}D^{\alpha}_{a+} f\right)(t) = f(t) - \sum_{k=0}^{n-1} \frac{f^{(k)}(a)}{k!}(t-a)^k. $$

Formula (1.1.9) may be regarded as the fractional counterpart of the classical fundamental theorem of calculus.

The next result establishes the connection between the Caputo and Riemann–Liouville derivatives.

Proposition 1.1.10 (Relation between Caputo and Riemann–Liouville derivatives) *For $n-1<\alpha<n$,*

$$D^{\alpha}_{a+}f(t) = {}^{C}D^{\alpha}_{a+}f(t) + \sum_{k=0}^{n-1} \frac{f^{(k)}(a)}{\Gamma(k+1-\alpha)}(t-a)^{k-\alpha}. \tag{1.1}$$

Equation (1.1) shows that the difference between the two fractional derivatives depends only on the initial values of the function and its derivatives.

Consequently, if

$$f^{(k)}(a) = 0, \qquad k = 0, 1, \ldots, n-1,$$

then the Caputo and Riemann–Liouville derivatives coincide:

$$D^{\alpha}_{a+}f(t) = {}^{C}D^{\alpha}_{a+}f(t).$$

1.1.6 Laplace transform techniques for fractional operators

The Laplace transform is one of the most powerful analytical tools for studying fractional differential equations. It transforms fractional differentiation and integration into algebraic operations in the complex domain, thereby simplifying the analysis and solution of fractional evolution equations.

Definition 1.1.11 (Laplace transform) *Let $f : [0,\infty) \to \mathbb{R}$ be a function of exponential order. Its Laplace transform is defined by*

$$\mathcal{L}\{f(t)\}(s) = F(s) = \int_0^{\infty} e^{-st} f(t)\, dt, \qquad s > 0.$$

The following theorem provides the Laplace transform of the Riemann–Liouville fractional integral.

Theorem 1.1.12 *[2, 14, 22] Let $\alpha > 0$. Then*

$$\mathcal{L}\left\{I^{\alpha}_{0+}f(t)\right\} = s^{-\alpha}F(s), \tag{1.2}$$

where $F(s) = \mathcal{L}\{f(t)\}$.

Equation (1.2) demonstrates that fractional integration corresponds to multiplication by $s^{-\alpha}$ in the Laplace domain.

The next result is fundamental for the analysis of fractional differential equations.

Theorem 1.1.13 (Laplace transform of the caputo derivative) *[2, 14, 22]*
Let $n-1 < \alpha \leq n$. *Then*

$$\mathcal{L}\left\{{}^{C}D^{\alpha}_{0+}f(t)\right\} = s^{\alpha}F(s) - \sum_{k=0}^{n-1} s^{\alpha-1-k} f^{(k)}(0). \tag{1.3}$$

For the important case $0 < \alpha < 1$, formula (1.3) simplifies to

$$\mathcal{L}\left\{{}^{C}D^{\alpha}_{0+}f(t)\right\} = s^{\alpha}F(s) - s^{\alpha-1}f(0). \tag{1.4}$$

Similarly, for $1 < \alpha < 2$, one obtains

$$\mathcal{L}\left\{{}^{C}D^{\alpha}_{0+}f(t)\right\} = s^{\alpha}F(s) - s^{\alpha-1}f(0) - s^{\alpha-2}f'(0). \tag{1.5}$$

The importance of formulas (1.4) and (1.5) lies in the fact that classical initial conditions appear explicitly in the transformed equation. This feature is one of the principal advantages of the Caputo derivative over other definitions of fractional derivatives.

To illustrate this idea, consider the fractional differential equation

$${}^{C}D^{\alpha}_{t}u(t) + \lambda u(t) = 0, \qquad u(0) = u_0.$$

Applying the Laplace transform and using (1.4) yields

$$s^{\alpha}U(s) - s^{\alpha-1}u_0 + \lambda U(s) = 0,$$

which can be rearranged as

$$U(s) = \frac{s^{\alpha-1}}{s^{\alpha}+\lambda}u_0.$$

This simple calculation illustrates how fractional differential equations can be transformed into algebraic equations in the Laplace domain. Such techniques play a central role in the theoretical analysis of fractional diffusion equations and will be employed repeatedly throughout this thesis.

1.2 The time-fractional diffusion equation

Fractional diffusion equations have become an important mathematical tool for describing anomalous transport phenomena in heterogeneous media. Unlike classical diffusion models, which are based on Brownian motion and lead to a linear growth of the mean square displacement with time, fractional diffusion models incorporate memory effects and are capable of describing subdiffusive processes observed in many physical and biological systems.

Examples include transport in porous media, groundwater flow, charge transport in disordered semiconductors, diffusion in biological tissues, and viscoelastic materials. In such situations, the classical diffusion equation often fails to accurately reproduce the observed dynamics, whereas fractional models provide a more realistic description through the introduction of nonlocal time derivatives.

In this thesis, we consider a time-fractional diffusion equation involving a spatially varying diffusion coefficient. This model constitutes the forward problem associated with the inverse coefficient identification problem studied in the subsequent chapters.

1.2.1 Mathematical model

Let $\Omega \subset \mathbb{R}^d$, with $d = 1, 2, 3$, be a bounded convex polyhedral domain with boundary $\partial\Omega$, and let $T > 0$ denote a fixed final time.

We consider the following initial-boundary value problem:

$$\partial_t^\alpha u(x,t) - \nabla \cdot (q(x)\nabla u(x,t)) = f(x,t), \qquad (x,t) \in \Omega \times (0,T], \tag{1.6}$$

subject to the initial condition

$$u(x,0) = u_0(x), \qquad x \in \Omega, \tag{1.7}$$

and the homogeneous Dirichlet boundary condition

$$u(x,t) = 0, \qquad (x,t) \in \partial\Omega \times (0,T]. \tag{1.8}$$

In this formulation,

- $u = u(x,t)$ denotes the state variable;
- $q = q(x)$ is the diffusion coefficient;
- $f = f(x,t)$ is a source term;
- u_0 is the prescribed initial condition;
- ∂_t^α denotes the Caputo fractional derivative of order $\alpha \in (0,1)$.

The Caputo derivative appearing in equation (1.6) is given by

$$\partial_t^\alpha u(x,t) = \frac{1}{\Gamma(1-\alpha)} \int_0^t (t-s)^{-\alpha} \frac{\partial u(x,s)}{\partial s}\, ds.$$

Unlike the classical time derivative, the Caputo derivative depends on the entire history of the solution over the interval $[0,t]$. Consequently, the evolution of the system at time t is influenced by its past states, reflecting the memory effect characteristic of many complex physical processes.

1.2.2 Physical interpretation

The fractional order α determines the strength of the memory effect. When $\alpha = 1$, the Caputo derivative reduces to the classical first-order derivative and equation (1.6) becomes

$$\frac{\partial u}{\partial t} - \nabla \cdot (q \nabla u) = f.$$

This is the standard diffusion equation governing Brownian motion. On the other hand, when $0 < \alpha < 1$, the diffusion process becomes slower than classical diffusion and exhibits memory effects. The mean square displacement satisfies

$$\langle x^2(t) \rangle \propto t^\alpha,$$

instead of the classical relation

$$\langle x^2(t) \rangle \propto t.$$

This phenomenon is known as subdiffusion.

Consequently, smaller values of α correspond to stronger memory effects and slower transport mechanisms.

1.2.3 Assumptions on the diffusion coefficient

Throughout this thesis, the diffusion coefficient is assumed to belong to an admissible set of physically meaningful parameters.

Definition 1.2.1 (Admissible diffusion coefficients) *Let $0 < c_0 < c_1$. The admissible set is defined by*

$$\mathcal{A} = \left\{ q \in H^1(\Omega) : c_0 \leq q(x) \leq c_1 \quad a.e. \ in \ \Omega \right\}. \tag{1.9}$$

The lower bound guarantees uniform ellipticity, while the upper bound ensures boundedness of the diffusion operator.

Indeed,

$$c_0|\xi|^2 \leq q(x)|\xi|^2 \leq c_1|\xi|^2, \qquad \forall \xi \in \mathbb{R}^d,$$

for almost every $x \in \Omega$.

These assumptions play a crucial role in establishing existence, uniqueness, and stability results.

1.2.4 Operator formulation

It is often convenient to rewrite the diffusion equation in an abstract operator form.

Define the elliptic operator

$$A(q)u = -\nabla \cdot (q(x)\nabla u)\,,$$

with domain

$$D(A) = H^2(\Omega) \cap H_0^1(\Omega).$$

Then equation (1.6) can be written compactly as

$$\partial_t^\alpha u + A(q)u = f, \qquad 0 < t \leq T.$$

The abstract formulation provides a convenient framework for spectral analysis and regularity theory.

1.2.5 Variational formulation

The weak formulation is obtained by multiplying equation (1.6) by a test function $v \in H_0^1(\Omega)$, and integrating over the spatial domain. This yields

$$\int_\Omega \partial_t^\alpha u\, v\, dx - \int_\Omega \nabla \cdot (q\nabla u)\, v\, dx = \int_\Omega f\, v\, dx. \tag{1.10}$$

Applying Green's formula to the diffusion term gives

$$-\int_\Omega \nabla \cdot (q\nabla u)\, v\, dx = \int_\Omega q\nabla u \cdot \nabla v\, dx - \int_{\partial\Omega} (q\nabla u \cdot n)\, v\, ds. \tag{1.11}$$

Since $v = 0 \quad$ on $\partial\Omega$, the boundary integral vanishes and equation (1.11) reduces to

$$-\int_\Omega \nabla \cdot (q\nabla u)\, v\, dx = \int_\Omega q\nabla u \cdot \nabla v\, dx. \tag{1.12}$$

Substituting (1.12) into (1.10) yields

$$\int_\Omega \partial_t^\alpha u\, v\, dx + \int_\Omega q\nabla u\cdot\nabla v\, dx = \int_\Omega f\, v\, dx.$$

Introducing the standard $L^2(\Omega)$ inner product

$$(u,v) = \int_\Omega u(x)v(x)\, dx,$$

the weak formulation can be stated as follows.

Definition 1.2.2 (Weak solution) *A function $u \in L^2(0,T;H_0^1(\Omega))$ is called a weak solution of problem (1.6)–(1.8) if*

$$(\partial_t^\alpha u(t), v) + (q\nabla u(t), \nabla v) = (f(t), v), \qquad \forall v \in H_0^1(\Omega),$$

for almost every $t \in (0,T]$, together with the initial condition (1.7).

The weak formulation constitutes the starting point for the well-posedness analysis of the forward problem and forms the basis for the finite element approximation developed in Chapter 3.

1.3 Existence and uniqueness of solution

Having established the variational formulation of the time-fractional diffusion equation, we now investigate the existence, uniqueness, and stability of weak solution. These results constitute the mathematical foundation of the forward problem and are essential for the analysis of the inverse coefficient identification problem developed in Chapter 2.

The analysis differs significantly from that of classical parabolic equations because the Caputo derivative is a nonlocal operator in time. Consequently, standard integration-by-parts arguments must be replaced by positivity properties specific to fractional derivatives.

Throughout this section, we assume that

- $$u_0 \in L^2(\Omega) \tag{1.13}$$

- $$f \in L^2\big(0,T;L^2(\Omega)\big) \tag{1.14}$$

- $$q \in \mathcal{A},\ \text{where } \mathcal{A}\text{denotes the admissible set defined in Section 1.3.} \tag{1.15}$$

1.3.1 Properties of the associated bilinear form

Define the bilinear form

$$a_q(u,v) = \int_\Omega q(x)\,\nabla u(x)\cdot\nabla v(x)\,dx, \qquad u,v \in H_0^1(\Omega).$$

The following properties are immediate consequences of the assumptions imposed on the diffusion coefficient.

Lemma 1.3.1 (Continuity) *There exists a constant $M > 0$ such that*

$$|a_q(u,v)| \le M\|u\|_{H^1(\Omega)}\|v\|_{H^1(\Omega)}, \qquad \forall u,v \in H_0^1(\Omega).$$

Proof. Using the upper bound $q(x) \le c_1$, together with the Cauchy–Schwarz inequality, we obtain

$$\begin{aligned}|a_q(u,v)| &= \left|\int_\Omega q\,\nabla u\cdot\nabla v\,dx\right| \\ &\le c_1\int_\Omega |\nabla u|\,|\nabla v|\,dx \\ &\le c_1\|\nabla u\|_{L^2(\Omega)}\|\nabla v\|_{L^2(\Omega)}.\end{aligned}$$

Using the equivalence of norms on $H_0^1(\Omega)$ yields the result. ■

Lemma 1.3.2 (Coercivity) *There exists a constant $\kappa > 0$ such that*

$$a_q(u,u) \ge \kappa\|u\|^2_{H^1(\Omega)}, \qquad \forall u \in H_0^1(\Omega).$$

Proof. Using the ellipticity condition $q(x) \geq c_0$, we obtain

$$a_q(u,u) = \int_\Omega q\,|\nabla u|^2\,dx \geq c_0\|\nabla u\|^2_{L^2(\Omega)}.$$

The Poincare inequality then implies

$$\|u\|_{H^1(\Omega)} \leq C\|\nabla u\|_{L^2(\Omega)},$$

which proves the result. ■

1.3.2 Positivity property of the caputo derivative

The key ingredient in the analysis of fractional diffusion equations is the positivity of the Caputo derivative.

Lemma 1.3.3 (Positivity property) *Let $v \in L^2\big(0,T;L^2(\Omega)\big)$ be sufficiently regular and satisfy $v(0)=0$. Then*

$$\int_0^T (\partial_t^\alpha v(t), v(t))\,dt \geq 0.$$

The positivity property plays the same role as the classical identity

$$\int_0^T (v'(t), v(t))\,dt = \frac{1}{2}\|v(T)\|^2_{L^2(\Omega)} - \frac{1}{2}\|v(0)\|^2_{L^2(\Omega)},$$

which is frequently used in the theory of parabolic equations.

1.3.3 Energy estimates

We now derive an a priori estimate for the solution. Let u be a weak solution of problem (1.6)–(1.8). Choosing $v = u(t)$ in the weak formulation yields

$$(\partial_t^\alpha u, u) + a_q(u,u) = (f,u).$$

Using the positivity property and coercivity of the bilinear form, we obtain

$$\kappa\|u\|_{H^1(\Omega)}^2 \leq (f,u).$$

Applying the Cauchy–Schwarz inequality gives

$$(f,u) \leq \|f\|_{L^2(\Omega)}\|u\|_{L^2(\Omega)}.$$

Using Young's inequality,

$$ab \leq \frac{\varepsilon}{2}a^2 + \frac{1}{2\varepsilon}b^2,$$

we obtain

$$\|u\|_{L^2(0,T;H_0^1(\Omega))} \leq C\left(\|u_0\|_{L^2(\Omega)} + \|f\|_{L^2(0,T;L^2(\Omega))}\right), \tag{1.16}$$

where the constant C is independent of u.

The estimate (1.16) is fundamental because it provides control of the solution in the natural energy space.

1.3.4 Existence of weak solutions

We are now in a position to establish the existence of weak solutions.

Theorem 1.3.4 (Existence) *[8, 9] Assume that conditions (1.13)–(1.15) hold. Then there exists at least one weak solution $u \in L^2\big(0,T;H_0^1(\Omega)\big)$ satisfying*

$$\partial_t^\alpha u \in L^2\big(0,T;H^{-1}(\Omega)\big).$$

Sketch of the Proof. The proof is based on the Galerkin method.

Let

$$V_m = \operatorname{span}\{\varphi_1,\ldots,\varphi_m\},$$

where $\{\varphi_k\}$ denotes the eigenfunctions of the elliptic operator.

We seek an approximate solution of the form

$$u_m(t) = \sum_{j=1}^{m} c_j(t)\varphi_j.$$

The Galerkin approximation satisfies a finite-dimensional fractional differential system. Using the a priori estimate (1.16), one obtains uniform bounds independent of m.

Compactness arguments and weak convergence then allow passage to the limit as $m \to \infty$, yielding a weak solution of the original problem. ■

1.3.5 Uniqueness of weak solutions

We now establish uniqueness.

Theorem 1.3.5 (Uniqueness) *[8, 9] Under the assumptions of the previous theorem, the weak solution of problem* (1.6)–(1.8) *is unique.*

Proof. Assume that u_1 and u_2 are two weak solutions corresponding to the same data. Define $w = u_1 - u_2$. Then w satisfies

$$\partial_t^\alpha w - \nabla \cdot (q \nabla w) = 0,$$

together with $w(x, 0) = 0$. Choosing $v = w$ in the weak formulation gives

$$(\partial_t^\alpha w, w) + a_q(w, w) = 0.$$

Using positivity and coercivity, we obtain $w = 0$. Hence $u_1 = u_2$, which proves uniqueness. ■

1.3.6 Continuous dependence on the data

The final ingredient of well-posedness is stability.

Theorem 1.3.6 (Continuous dependence) *[8, 9] Let $(u_0^{(1)}, f^{(1)})$ and $(u_0^{(2)}, f^{(2)})$ be two sets of data with corresponding solutions $u^{(1)}$ and $u^{(2)}$. Then*

$$\|u^{(1)} - u^{(2)}\|_{L^2(0,T;H_0^1(\Omega))} \leq C\Big(\|u_0^{(1)} - u_0^{(2)}\|_{L^2(\Omega)} + \|f^{(1)} - f^{(2)}\|_{L^2(0,T;L^2(\Omega))}\Big).$$

,

Therefore, small perturbations in the initial condition or source term produce only small variations in the solution.

Combining existence, uniqueness, and continuous dependence, we conclude that the time-fractional diffusion equation is well posed in the sense of Hadamard.

1.4 Regularity results

In the previous section, we established the existence and uniqueness of weak solutions for the time-fractional diffusion equation. We now investigate the regularity properties of these solutions. Regularity analysis is fundamental for both theoretical and computational purposes. On the one hand, it provides deeper insight into the qualitative behavior of solutions. On the other hand, it forms the basis for the derivation of convergence rates and error estimates for numerical methods.

Unlike classical parabolic equations, time-fractional diffusion equations exhibit only limited smoothing properties due to the nonlocal nature of the Caputo derivative. Consequently, the regularity of solutions is strongly influenced by the regularity of the initial data, the source term, and the fractional order α.

Throughout this section, we assume that

$$u_0 \in H^2(\Omega) \cap H_0^1(\Omega),$$

and

$$f \in C^1\big([0,T]; L^2(\Omega)\big).$$

Moreover, the diffusion coefficient is assumed to satisfy

$$q \in W^{1,\infty}(\Omega) \cap \mathcal{A}.$$

Under these assumptions, the solution enjoys improved spatial and temporal regularity.

1.4.1 Limited smoothing property

Time-fractional diffusion equations exhibit limited smoothing properties compared with classical parabolic equations [8, 9] where the solution operator generates an analytic semigroup and therefore possesses a strong smoothing effect. In particular, even if the initial data belong only to $L^2(\Omega)$, the solution becomes infinitely differentiable for every positive time.

In contrast, the solution of a fractional diffusion equation gains regularity much more slowly. To illustrate this phenomenon, consider the homogeneous problem

$$\partial_t^\alpha u + Au = 0, \qquad u(0) = u_0,$$

where

$$A = -\nabla \cdot (q\nabla).$$

The solution admits the spectral representation

$$u(t) = \sum_{k=1}^{\infty} E_\alpha\left(-\lambda_k t^\alpha\right)\left(u_0, \varphi_k\right)\varphi_k,$$

where

$$E_\alpha(z) = \sum_{m=0}^{\infty} \frac{z^m}{\Gamma(\alpha m + 1)}$$

denotes the Mittag–Leffler function.

Remark 1.4.1 *The Mittag–Leffler function plays the same role in fractional evolution equations as the exponential function does in classical diffusion equations. Since its decay* *is slower than that of the exponential function, the regularization effect of the fractional diffusion equation is correspondingly weaker.*

1.4.2 Spatial regularity

We first investigate the spatial smoothness of the solution.

Theorem 1.4.2 (Spatial regularity) *[9] Let u be the solution of problem (1.6)–(1.8). Then there exists a constant $C > 0$ such that*

$$\|u(t)\|_{H^2(\Omega)} \leq C \left(\|u_0\|_{H^2(\Omega)} + \|f\|_{L^\infty(0,T;L^2(\Omega))} \right),$$

for every $t \in (0, T]$.

The estimate (1.4.2) shows that the solution inherits the spatial regularity of the data. More generally, if

$$u_0 \in D(A^\sigma), \qquad 0 \leq \sigma \leq 1,$$

then

$$u(t) \in D(A^\sigma), \qquad t > 0.$$

Therefore, the smoothness of the solution is closely connected to the fractional powers of the elliptic operator introduced in Section 1.2.

1.4.3 Temporal regularity

We now turn to the regularity of the solution with respect to time. Unlike the classical diffusion equation, the time derivative of a fractional diffusion solution generally exhibits singular behavior near the initial time.

Theorem 1.4.3 (Temporal regularity) *[9] Let u be the solution of the fractional diffusion equation. Then there exists a constant $C > 0$ such that*

$$\|u'(t)\|_{L^2(\Omega)} \leq C\, t^{\alpha-1}, \qquad 0 < t \leq T. \tag{1.17}$$

Since

$$\alpha - 1 < 0, \qquad 0 < \alpha < 1,$$

the estimate (1.17) becomes singular as $t \to 0^+$. This behavior is fundamentally different from the classical heat equation and reflects the memory effect associated with the fractional derivative. Higher-order temporal derivatives satisfy similar estimates. In particular,

$$\|u''(t)\|_{L^2(\Omega)} \leq C\, t^{\alpha-2}, \qquad 0 < t \leq T.$$

Consequently, the solution is generally less regular near the initial time than solutions of classical parabolic equations.

1.4.4 Maximal regularity estimates

An important class of estimates concerns the simultaneous control of spatial and temporal derivatives [10, 11].

Theorem 1.4.4 (Maximal regularity) *[11] Assume that $u_0 = 0$. Then the solution satisfies*

$$\|\partial_t^\alpha u\|_{L^2(0,T;L^2(\Omega))} + \|Au\|_{L^2(0,T;L^2(\Omega))} \leq C\|f\|_{L^2(0,T;L^2(\Omega))}. \tag{1.18}$$

Estimate (1.18) plays a central role in the numerical analysis of fractional diffusion equations and will be used later in the derivation of error estimates.

Chapter 2

Inverse Problem Analysis

2.1 Problem formulation

In Chapter 1, we established the well-posedness of the forward time-fractional diffusion problem and analyzed the dependence of the solution on the diffusion coefficient. We now consider the corresponding inverse problem, whose objective is to reconstruct the unknown space-dependent diffusion coefficient from observational data.

Inverse problems arise in many applications where certain physical parameters cannot be measured directly and must instead be inferred from observable quantities. In diffusion processes, the diffusion coefficient characterizes the transport properties of the medium and plays a fundamental role in determining the evolution of the state variable. Determining this coefficient from experimental or simulated observations is therefore of considerable practical and theoretical interest.

Let $\Omega \subset \mathbb{R}^d$, with $d = 1, 2, 3$, be a bounded domain with sufficiently smooth boundary $\partial\Omega$, and let $T > 0$ denote a fixed final time. We consider the time-fractional diffusion equation

$$\partial_t^\alpha u(x,t) - \nabla \cdot (q(x)\nabla u(x,t)) = f(x,t), \qquad (x,t) \in \Omega \times (0,T], \tag{2.1}$$

subject to the homogeneous Dirichlet boundary condition

$$u(x,t) = 0, \qquad (x,t) \in \partial\Omega \times (0,T], \tag{2.2}$$

and the initial condition

$$u(x,0) = u_0(x), \qquad x \in \Omega. \tag{2.3}$$

The unknown parameter is the spatially varying diffusion coefficient $q(x)$, which is assumed to belong to the admissible set

$$\mathcal{A} = \left\{ q \in H^1(\Omega) : 0 < q_{\min} \leq q(x) \leq q_{\max} \quad \text{a.e. in } \Omega \right\}.$$

Let $q^\dagger \in \mathcal{A}$ denote the exact diffusion coefficient and let

$$u^\dagger = u(q^\dagger)$$

be the corresponding solution of the forward problem.

In practice, the exact solution is not available. Instead, one has access to noisy measurements

$$z^\delta = u^\dagger + \xi,$$

where ξ represents measurement noise satisfying

$$|z^\delta - u^\dagger|_{L^2(0,T;L^2(\Omega))} \leq \delta,$$

for some noise level $\delta > 0$.

The inverse problem can now be stated as follows.

Inverse problem. Given the noisy observations z^δ, determine the diffusion coefficient $q^\dagger$ such that the corresponding solution of the time-fractional diffusion equation reproduces the measured data.

To formulate the inverse problem in an operator framework, we introduce the parameter-to-state map

$$F : \mathcal{A} \to L^2(0, T; L^2(\Omega)), \qquad F(q) = u(q),$$

where $u(q)$ denotes the unique weak solution associated with the diffusion coefficient q.

Using this notation, the inverse problem may be written as the nonlinear operator equation

$$F(q) = z^\delta. \tag{2.4}$$

The analysis of this problem constitutes the main objective of this chapter. As will be shown in the next section, the inverse problem is generally ill posed and therefore requires the introduction of suitable regularization techniques to obtain stable and reliable reconstructions.

2.2 Ill-posedness of the inverse problem

The inverse problem formulated in the previous section consists of determining the space-dependent diffusion coefficient $q(x)$ from measurements of the corresponding state variable. In operator form, this problem can be written as

$$F(q) = z^\delta, \tag{2.5}$$

where F denotes the parameter-to-state map and z^δ represents the available observational data.

Although the associated forward problem is well posed, the inverse problem generally does not possess the same stability properties. Indeed, inverse coefficient problems for diffusion equations are typically ill posed in the sense that small perturbations in the observational data may lead to large variations in the reconstructed coefficient. Consequently, direct inversion of the operator equation (2.5) is generally unstable.

The origin of this instability lies in the smoothing nature of diffusion processes. During the evolution of the system, fine-scale information concerning the unknown coefficient is partially lost, while measurement errors are inevitably introduced into the observed data. As a result, different diffusion coefficients may produce very similar observations, making the reconstruction process highly sensitive to noise.

To illustrate this phenomenon, consider two observational data sets z_1 and z_2 satisfying

$$|z_1 - z_2|_{L^2(0,T;L^2(\Omega))} \ll 1.$$

Let q_1 and q_2 denote the corresponding reconstructed coefficients. In a stable inverse problem, one would expect the difference between the reconstructed coefficients to remain proportional to the perturbation in the data. However, this property generally fails for inverse diffusion problems, where even small measurement errors may lead to significant changes in the reconstructed coefficient.

This behavior can be understood from the compactness properties of the parameter-to-state map. The forward operator smooths irregularities in the coefficient and transforms local variations of the parameter into relatively small variations of the observable state. Consequently, recovering the coefficient from the observations amounts to inverting a smoothing operator, a process that is inherently unstable.

From a practical viewpoint, measurement data are always contaminated by noise. If the inverse problem is solved without stabilization, the reconstructed coefficient may exhibit strong oscillations or unrealistic values that do not correspond to the physical properties of the medium. Therefore, additional information concerning the unknown coefficient must be incorporated into the reconstruction procedure.

To overcome this difficulty, regularization techniques are employed. These methods replace the original ill-posed inverse problem by a nearby optimization problem possessing improved stability properties. Among the many regularization techniques available in the literature, Tikhonov regularization is one of the most widely used due to its simplicity, robustness, and strong theoretical foundations.

The main idea of Tikhonov regularization is to balance two competing objectives.

On the one hand, the reconstructed coefficient should reproduce the measured data as accurately as possible. On the other hand, the reconstruction should satisfy certain regularity requirements reflecting prior knowledge about the unknown parameter. This approach leads to stable approximations and provides a rigorous framework for both theoretical analysis and numerical reconstruction.

In the following sections, we investigate the analytical properties of the parameter-to-state map and develop a Tikhonov regularization framework for the stable recovery of the diffusion coefficient.

2.3 Analysis of the parameter-to-state map

The parameter-to-state map establishes the relationship between the unknown diffusion coefficient and the corresponding solution of the forward problem. Its analytical properties play a central role in the study of the inverse problem. In particular, continuity is required for the existence of regularized solutions, while differentiability is essential for deriving sensitivity relations and optimization procedures.

Recall that the admissible set is defined by

$$\mathcal{A} = \left\{ q \in H^1(\Omega) : 0 < q_{\min} \le q(x) \le q_{\max} \quad \text{a.e. in } \Omega \right\}.$$

For every coefficient $q \in \mathcal{A}$, the forward problem admits a unique weak solution according to the results established in Chapter 1. Consequently, the parameter-to-state map

$$F : \mathcal{A} \to L^2(0,T;L^2(\Omega)), \qquad q \mapsto u(q),$$

is well defined.

The study of the inverse problem relies heavily on the analytical behavior of this operator. We therefore investigate its continuity and differentiability properties.

2.3.1 Continuity of the parameter-to-state map

The first property required in the analysis of the inverse problem is the continuous dependence of the solution on the diffusion coefficient.

Theorem 2.3.1 *[12]*

Let $\{q_n\} \subset \mathcal{A}$ be a sequence such that

$$q_n \to q \qquad \textit{in } H^1(\Omega).$$

Then the corresponding solutions satisfy

$$u(q_n) \to u(q) \qquad \textit{in } L^2(0,T;L^2(\Omega)).$$

Hence, the parameter-to-state map F is continuous on $\mathcal{A}$.

Proof.

Let

$$w_n = u(q_n) - u(q).$$

The functions $u(q_n)$ and $u(q)$ satisfy

$$\partial_t^\alpha u(q_n) - \nabla \cdot (q_n \nabla u(q_n)) = f,$$

and

$$\partial_t^\alpha u(q) - \nabla \cdot (q \nabla u(q)) = f.$$

Subtracting the two equations yields

$$\partial_t^\alpha w_n - \nabla \cdot (q_n \nabla w_n) = \nabla \cdot ((q_n - q)\nabla u(q)).$$

Using the stability estimate established for the forward problem and the convergence

$$q_n \to q \qquad \text{in } H^1(\Omega),$$

we obtain

$$|w_n|_{L^2(0,T;L^2(\Omega))} \longrightarrow 0.$$

Therefore,

$$u(q_n) \to u(q) \qquad \text{in } L^2(0,T;L^2(\Omega)),$$

which proves the continuity of the parameter-to-state map.

■

The continuity of the parameter-to-state map guarantees that small perturbations of the diffusion coefficient produce small variations in the corresponding state variable. This property is essential for establishing the existence of regularized solutions.

2.3.2 Fréchet differentiability of the parameter-to-state map

To derive sensitivity relations and optimization procedures, it is necessary to investigate the differentiability of the parameter-to-state map.

Let $q \in \mathcal{A}$ and let $h \in H^1(\Omega)$ be an admissible perturbation. For sufficiently small ε, define

$$q_\varepsilon = q + \varepsilon h.$$

The corresponding state solution is denoted by

$$u_\varepsilon = u(q_\varepsilon).$$

The first-order variation of the state with respect to perturbations of the diffusion coefficient is characterized by the following result.

Theorem 2.3.2 *[7]*

The parameter-to-state map

$$F : \mathcal{A} \to L^2(0,T; L^2(\Omega))$$

is Fréchet differentiable .

Moreover, for every perturbation direction h, the derivative

$$F'(q)h$$

is given by the solution of the sensitivity problem

$$\partial_t^\alpha w - \nabla \cdot (q\nabla w) = \nabla \cdot (h\nabla u), \qquad (x,t) \in \Omega \times (0,T],$$

subject to

$$w(x,t) = 0, \qquad (x,t) \in \partial\Omega \times (0,T],$$

and

$$w(x,0) = 0, \qquad x \in \Omega,$$

where $u = u(q)$ denotes the solution of the forward problem corresponding to the coefficient q.

Proof.

Let

$$u_\varepsilon = u(q + \varepsilon h)$$

be the solution associated with the perturbed coefficient.

The perturbed state satisfies

$$\partial_t^\alpha u_\varepsilon - \nabla \cdot \big((q + \varepsilon h)\nabla u_\varepsilon\big) = f.$$

Subtracting the forward equation satisfied by

$$u = u(q)$$

gives

$$\partial_t^\alpha (u_\varepsilon - u) - \nabla \cdot \big(q \nabla (u_\varepsilon - u)\big) = \varepsilon \nabla \cdot (h \nabla u_\varepsilon).$$

Define

$$w_\varepsilon = \frac{u_\varepsilon - u}{\varepsilon}.$$

Dividing by ε yields

$$\partial_t^\alpha w_\varepsilon - \nabla \cdot (q \nabla w_\varepsilon) = \nabla \cdot (h \nabla u_\varepsilon).$$

Using the continuity result established previously, we have

$$u_\varepsilon \to u$$

as

$$\varepsilon \to 0.$$

Passing to the limit therefore gives

$$\partial_t^\alpha w - \nabla \cdot (q \nabla w) = \nabla \cdot (h \nabla u).$$

Standard stability estimates for the forward problem show that the remainder term is of order $o(\varepsilon)$, which proves the Fréchet differentiability of the parameter-to-state map.

■

The derivative $F'(q)$ is commonly referred to as the sensitivity operator. It quantifies the influence of perturbations of the diffusion coefficient on the observable state and plays a fundamental role in the derivation of optimality conditions and reconstruction algorithms.

The continuity and differentiability properties established above constitute the principal analytical tools required for the study of the regularized inverse problem developed in the following sections.

2.4 Tikhonov regularization

As discussed in the previous section, the inverse problem of recovering the diffusion coefficient from observational data is generally ill posed. In particular, direct inversion of the parameter-to-state map is unstable with respect to measurement errors. To obtain stable and reliable reconstructions, regularization techniques must be employed.

In this work, we adopt the classical Tikhonov regularization framework, which transforms the inverse problem into a constrained optimization problem. The main idea is to balance the agreement with the measured data and the smoothness of the reconstructed coefficient.

2.4.1 The Tikhonov functional

Let

$$z^\delta \in L^2(0,T;L^2(\Omega))$$

denote the noisy observational data satisfying

$$|z^\delta - z^\dagger|_{L^2(0,T;L^2(\Omega))} \leq \delta,$$

where

$$z^\dagger = F(q^\dagger)$$

represents the exact observation associated with the exact diffusion coefficient $q^\dagger$.

The discrepancy between the predicted observations and the measured data is quantified through the least-squares functional

$$\Phi(q) = \frac{1}{2}|F(q) - z^\delta|^2_{L^2(0,T;L^2(\Omega))}.$$

To stabilize the reconstruction process, we introduce the regularization term

$$R(q) = \frac{1}{2}|\nabla q|^2_{L^2(\Omega)},$$

which penalizes highly oscillatory diffusion coefficients and promotes smooth solutions. Combining the data fidelity and regularization terms leads to the Tikhonov functional

$$J_\gamma(q) = \frac{1}{2}|F(q) - z^\delta|^2_{L^2(0,T;L^2(\Omega))} + \frac{\gamma}{2}|\nabla q|^2_{L^2(\Omega)}, \tag{2.6}$$

where $\gamma > 0$ denotes the regularization parameter.

The first term measures the discrepancy between the model prediction and the observations, while the second term incorporates prior smoothness information on the unknown coefficient.

The regularization parameter controls the balance between data fitting and smoothness. Small values of γ place greater emphasis on fitting the measurements, whereas larger values promote smoother reconstructions.

2.4.2 The regularized inverse problem

The regularized reconstruction of the diffusion coefficient is formulated as the minimization problem

$$\min_{q \in \mathcal{A}} J_\gamma(q), \tag{2.7}$$

where $\mathcal{A}$ denotes the admissible set introduced in Section 2.1.

The optimization problem (2.7) replaces the original ill-posed inverse problem by a stable variational formulation.

Definition 2.4.1 *A coefficient $q_\gamma^\delta \in \mathcal{A}$ is called a* Tikhonov regularized solution *if*

$$J_\gamma(q_\gamma^\delta) = \min_{q\in\mathcal{A}} J_\gamma(q).$$

The regularized solution provides a stable approximation of the exact diffusion coefficient even when the observational data are contaminated by noise.

2.4.3 Existence of minimizers

We now establish the existence of solutions to the regularized optimization problem.

Theorem 2.4.2 *[12]*

For every $\gamma > 0$ and every data set

$$z^\delta \in L^2(0,T;L^2(\Omega)),$$

the minimization problem (2.7) admits at least one solution

$$q_\gamma^\delta \in \mathcal{A}.$$

Proof.

Let $\{q_n\} \subset \mathcal{A}$ be a minimizing sequence satisfying

$$J_\gamma(q_n) \to \inf_{q\in\mathcal{A}} J_\gamma(q).$$

Since the Tikhonov functional contains the regularization term

$$\frac{\gamma}{2}|\nabla q_n|^2_{L^2(\Omega)},$$

the sequence $\{q_n\}$ is bounded in $H^1(\Omega)$.

Therefore, there exists a subsequence, still denoted by $\{q_n\}$, and an element

$$\bar{q} \in H^1(\Omega)$$

such that

$$q_n \rightharpoonup \bar{q} \qquad \text{in } H^1(\Omega).$$

Since the admissible set $\mathcal{A}$ is closed and convex, it follows that

$$\bar{q} \in \mathcal{A}.$$

Furthermore, by the continuity of the parameter-to-state map established in Theorem 2.3.1, together with the weak lower semicontinuity of the H^1 seminorm, we obtain

$$J_\gamma(\bar{q}) \leq \liminf_{n\to\infty} J_\gamma(q_n).$$

Consequently, $\bar{q}$ minimizes the functional J_γ over $\mathcal{A}$, proving the existence of a regularized solution.

■

The existence theorem provides the mathematical foundation for the reconstruction procedure. It guarantees that the regularized inverse problem possesses at least one solution and justifies the optimization approach adopted throughout this work.

2.5 Stability and convergence of Tikhonov regularization

In the previous section, we established the existence of minimizers for the regularized inverse problem. We now investigate their stability and asymptotic behavior as the noise level decreases. These results provide the theoretical justification for the regularization approach and guarantee that increasingly accurate measurements lead to increasingly accurate reconstructions.

Let $q^\dagger \in \mathcal{A}$ denote the exact diffusion coefficient and let

$$z^\dagger = F(q^\dagger)$$

be the corresponding exact observation.

The noisy measurements are assumed to satisfy

$$|z^{\delta} - z^{\dagger}|_{L^2(0,T;L^2(\Omega))} \leq \delta, \tag{2.8}$$

where $\delta > 0$ denotes the noise level.

2.5.1 Stability of regularized solutions

A fundamental requirement of any regularization method is stability with respect to perturbations in the observational data.

Theorem 2.5.1 (Stability) *[12]*

Let $\{z_n^{\delta}\}$ be a sequence of observational data satisfying

$$z_n^{\delta} \to z^{\delta} \qquad \text{in } L^2(0,T;L^2(\Omega)),$$

and let q_n be corresponding minimizers of the Tikhonov functional

$$J_{\gamma}(q) = \frac{1}{2}|F(q) - z_n^{\delta}|^2 + \frac{\gamma}{2}|\nabla q|^2.$$

Then there exist a subsequence, still denoted by $\{q_n\}$, and an element $q^* \in \mathcal{A}$ such that

$$q_n \rightharpoonup q^* \qquad \text{in } H^1(\Omega).$$

Moreover, q^* is a minimizer associated with the limiting data z^{δ}

Proof.

Since each q_n minimizes the Tikhonov functional, the regularization term yields a uniform bound in $H^1(\Omega)$. Consequently, the sequence $\{q_n\}$ is bounded in $H^1(\Omega)$.

By weak compactness, there exists a subsequence converging weakly to some $q^* \in H^1(\Omega)$. Since the admissible set is closed and convex, we have $q^* \in \mathcal{A}$.

The continuity of the parameter-to-state map and the weak lower semicontinuity of the regularization term allow passage to the limit in the Tikhonov functional, showing that q^* is a minimizer corresponding to the limiting data.

■

The theorem shows that small perturbations in the measurements cannot produce arbitrarily large changes in the regularized reconstruction, thereby restoring stability to the inverse problem.

2.5.2 A fundamental estimate

The following estimate plays a central role in the convergence analysis.

Lemma 2.5.2 *Let q_γ^δ be a minimizer of the Tikhonov functional. Then*

$$J_\gamma(q_\gamma^\delta) \leq J_\gamma(q^\dagger).$$

Consequently,

$$\frac{1}{2}|F(q_\gamma^\delta) - z^\delta|^2_{L^2(0,T;L^2(\Omega))} + \frac{\gamma}{2}|\nabla q_\gamma^\delta|^2_{L^2(\Omega)} \leq \frac{\delta^2}{2} + \frac{\gamma}{2}|\nabla q^\dagger|^2_{L^2(\Omega)}. \tag{2.9}$$

Proof.

Since q_γ^δ minimizes the Tikhonov functional,

$$J_\gamma(q_\gamma^\delta) \leq J_\gamma(q^\dagger).$$

Using

$$F(q^\dagger) = z^\dagger$$

and the noise estimate (2.8), we obtain

$$|F(q^\dagger) - z^\delta| = |z^\dagger - z^\delta| \leq \delta.$$

Substituting this inequality into the definition of the Tikhonov functional immediately yields (2.9).

■

The estimate implies that the family of regularized solutions remains uniformly bounded in $H^1(\Omega)$, which provides the compactness required in the convergence analysis.

2.5.3 Convergence of regularized solutions

We now establish the main convergence theorem.

Theorem 2.5.3 (Convergence of Tikhonov regularization) *[12]*

Assume that the regularization parameters satisfy

$$\gamma_n \to 0,$$

and

$$\frac{\delta_n^2}{\gamma_n} \to 0, \tag{2.10}$$

as $n \to \infty$.

Let q_n *denote a sequence of minimizers corresponding to noise levels* δ_n *and regularization parameters* γ_n.

Then there exist a subsequence and an element $\bar{q} \in \mathcal{A}$ *such that*

$$q_n \rightharpoonup \bar{q} \qquad \text{in } H^1(\Omega).$$

Moreover,

$$F(\bar{q}) = z^\dagger.$$

Therefore, $\bar{q}$ *is a solution of the exact inverse problem.*

Proof.

From Lemma 2.5.2, the sequence $\{q_n\}$ is bounded in $H^1(\Omega)$. Hence, there exists a subsequence converging weakly to some $\bar{q} \in \mathcal{A}$.

Using estimate (2.9) together with the assumptions

$$\gamma_n \to 0, \qquad \frac{\delta_n^2}{\gamma_n} \to 0,$$

it follows that

$$|F(q_n) - z^{\delta_n}| \to 0.$$

Since

$$z^{\delta_n} \to z^\dagger,$$

we obtain

$$F(q_n) \to z^\dagger.$$

The continuity of the parameter-to-state map then yields

$$F(\bar{q}) = z^\dagger.$$

Therefore, $\bar{q}$ satisfies the exact inverse problem and is an exact solution corresponding to the noiseless observation data.

■

The convergence theorem establishes the consistency of the regularization method. As the measurement noise tends to zero and the regularization parameter is chosen appropriately, the regularized solutions converge to a solution of the exact inverse problem.

2.6 Identifiability of the diffusion coefficient

The convergence results established in the previous section guarantee that regularized solutions approach solutions of the exact inverse problem as the noise level tends to zero. However, convergence alone does not ensure recovery of the true diffusion coefficient. This question is closely related to the notion of identifiability.

Identifiability concerns the uniqueness of the reconstruction process. More precisely, it addresses whether the available observations contain sufficient information to uniquely determine the unknown parameter. If identifiability fails, different diffusion coefficients may generate identical observations, making unique reconstruction impossible regardless of the quality of the data.

2.6.1 Definition of identifiability

Recall that the parameter-to-state map is defined by

$$F : \mathcal{A} \to L^2(0,T; L^2(\Omega)), \qquad q \mapsto u(q).$$

Definition 2.6.1 *The diffusion coefficient is said to be identifiable if*

$$F(q_1) = F(q_2)$$

implies

$$q_1 = q_2 \qquad a.e. \ in \ \Omega.$$

In other words, different diffusion coefficients produce different observable states.

When identifiability holds, the inverse problem admits at most one exact solution.

2.6.2 A uniqueness result

The following theorem provides a uniqueness principle for the reconstruction of the diffusion coefficient.

Theorem 2.6.2 *[3, 13]*

Let $q_1, q_2 \in \mathcal{A}$ and let

$$u_1 = u(q_1), \qquad u_2 = u(q_2)$$

denote the corresponding solutions of the time-fractional diffusion equation. Assume that

$$u_1(x,t) = u_2(x,t), \qquad (x,t) \in \Omega \times (0,T),$$

and suppose that the solution satisfies a suitable nondegeneracy condition.

Then

$$q_1(x) = q_2(x) \qquad a.e. \ in \ \Omega.$$

Proof. Formal argument

Assume that two admissible diffusion coefficients produce identical observations. Since

$$u_1 = u_2,$$

the corresponding governing equations satisfy

$$\partial_t^\alpha u - \nabla \cdot (q_1 \nabla u) = f,$$

and

$$\partial_t^\alpha u - \nabla \cdot (q_2 \nabla u) = f.$$

Subtracting the two equations yields

$$\nabla \cdot \big((q_1 - q_2)\nabla u\big) = 0.$$

Under a suitable nondegeneracy assumption on the solution u, it follows that

$$q_1 - q_2 = 0 \qquad \text{a.e. in } \Omega.$$

Therefore,

$$q_1 = q_2 \qquad \text{a.e. in } \Omega.$$

This establishes uniqueness of the reconstructed diffusion coefficient.

■

The uniqueness result shows that, under suitable assumptions, the available observations contain sufficient information to determine the unknown diffusion coefficient uniquely. Consequently, the inverse problem admits a unique exact solution. Combined with the convergence results established in the previous section, this implies that the regularized reconstructions approach the true coefficient as the noise level tends to zero.

Chapter 3

Numerical approximation and reconstruction method

3.1 Introduction

This chapter presents the numerical framework used for the reconstruction of the space-dependent diffusion coefficient in the time-fractional diffusion equation. Since analytical solutions are generally unavailable, numerical methods are required for both the forward and inverse problems.

The proposed approach combines the finite element method for the spatial discretization with convolution quadrature for the approximation of the Caputo fractional derivative. This leads to a fully discrete forward problem that can be efficiently solved for a given diffusion coefficient.

The inverse problem is formulated as the minimization of a discrete Tikhonov functional. The resulting optimization problem is solved using the Nelder–Mead simplex algorithm, a derivative-free method particularly suitable for nonlinear inverse problems.

The chapter first presents the spatial and temporal discretizations, followed by the fully discrete formulation of the forward problem. The discrete inverse problem and the reconstruction strategy are then introduced, together with the optimization algorithm and implementation details used in the numerical experiments.

3.2 Spatial discretization by the finite element method

The first step in the numerical approximation of the forward problem consists of discretizing the spatial domain. In this work, the finite element method is employed due to its flexibility in handling variational formulations and complex geometries. The method provides an accurate approximation of the state variable while naturally incorporating the weak formulation developed in Chapter 1.

3.2.1 Triangulation of the domain

Let $\Omega \subset \mathbb{R}^d$, with $d = 1, 2, 3$, be a bounded polygonal domain. For a mesh parameter $h > 0$, let

$$\mathcal{T}_h = \{K\}$$

denote a conforming triangulation of Ω.

The mesh size is defined by

$$h = \max_{K \in \mathcal{T}_h} \operatorname{diam}(K).$$

Throughout this chapter, the triangulations are assumed to be shape-regular and quasi-uniform. These assumptions guarantee the approximation properties required for the finite element analysis.

3.2.2 Finite element space

Let $P_1(K)$ denote the space of polynomials of degree at most one on an element K. The finite element space is defined by

$$X_h = \left\{ v_h \in C(\overline{\Omega}) : v_h|_K \in P_1(K), \quad \forall K \in \mathcal{T}_h \right\}.$$

To incorporate the homogeneous Dirichlet boundary condition, we introduce

$$X_h^0 = X_h \cap H_0^1(\Omega).$$

The numerical approximation of the state variable will be sought in the finite-dimensional space X_h^0.

Let

$$\{\varphi_1, \varphi_2, \dots, \varphi_M\}$$

be the standard nodal basis of X_h^0. Every function $v_h \in X_h^0$ admits the representation

$$v_h(x) = \sum_{j=1}^{M} v_j \varphi_j(x),$$

where $\{v_j\}_{j=1}^M$ are the corresponding nodal coefficients.

3.2.3 Approximation of the diffusion coefficient

The unknown parameter of the inverse problem is the space-dependent diffusion coefficient $q(x)$. Its finite element approximation is denoted by

$$q_h \in A_h,$$

where

$$A_h = X_h.$$

The corresponding discrete admissible set is defined by

$$\mathcal{A}_h = \{ q_h \in A_h : q_{\min} \le q_h(x) \le q_{\max}, \quad \forall x \in \Omega \}.$$

The finite-dimensional representation of the coefficient transforms the inverse problem into a finite-dimensional optimization problem.

Using the finite element basis, the coefficient approximation can be expressed as

$$q_h(x) = \sum_{j=1}^{M} q_j \varphi_j(x),$$

where the coefficients $\{q_j\}_{j=1}^{M}$ constitute the unknown parameters to be determined from the observational data.

3.2.4 Time discretization by convolution quadrature

To approximate the Caputo fractional derivative of order α, we employ Lubich's convolution quadrature method based on the backward Euler scheme. This approach is particularly suitable for fractional diffusion problems since it naturally incorporates the memory effects associated with fractional operators.

Let

$$0 = t_0 < t_1 < \cdots < t_N = T$$

be a uniform partition of the time interval $[0, T]$ with time step

$$\tau = \frac{T}{N}.$$

The convolution quadrature method approximates the fractional derivative at each time level using a weighted combination of the current and all previous solution values. Consequently, the nonlocal nature of the fractional derivative is preserved in the discrete model.

Combined with the finite element approximation introduced in the previous section, convolution quadrature yields a stable and consistent discretization of the forward problem. The resulting scheme provides approximations of the solution at all discrete time levels and forms the basis of the reconstruction procedure.

3.2.5 Fully discrete approximation of the forward problem

The finite element discretization in space and the convolution quadrature approximation in time lead to a fully discrete formulation of the time-fractional diffusion equation.

For a given approximation of the diffusion coefficient q_h, the fully discrete problem consists of computing the numerical solution

$$U_h^n \in X_h^0, \qquad n = 1, \ldots, N,$$

at each time level.

The fully discrete variational formulation reads

$$(\bar{\partial}_\tau^\alpha U_h^n, \chi_h) + (q_h \nabla U_h^n, \nabla \chi_h) = (f^n, \chi_h), \qquad \forall \chi_h \in X_h^0,$$

for $n = 1, \ldots, N$, together with the discrete initial condition

$$U_h^0 = P_h u_0,$$

where P_h denotes the L^2-projection onto X_h^0.

The solution is obtained recursively, with the approximation at a given time level depending on all previously computed states. This reflects the memory effect inherent in fractional diffusion models.

The resulting numerical scheme admits a unique discrete solution and provides a stable approximation of the forward problem. During the reconstruction process, the forward solver is repeatedly used to evaluate the model response corresponding to different coefficient distributions.

3.2.6 Discrete Tikhonov formulation of the inverse problem

The inverse problem consists of reconstructing the space-dependent diffusion coefficient from noisy observations of the state variable. After discretization of the forward problem, the reconstruction is formulated as a finite-dimensional optimization problem.

Let

$$q_h \in \mathcal{A}_h$$

denote a finite element approximation of the unknown diffusion coefficient and let

$$U_h(q_h) = \{U_h^n(q_h)\}_{n=1}^N$$

be the corresponding solution of the fully discrete forward problem.

Furthermore, let

$$Z^\delta = \{Z_\delta^n\}_{n=1}^N$$

denote the available observation data.

To stabilize the reconstruction process, we consider the discrete Tikhonov functional

$$J_{\gamma,h}(q_h) = \frac{1}{2}\sum_{n=1}^{N} \tau |U_h^n(q_h) - Z_\delta^n|_{L^2(\Omega)}^2 + \frac{\gamma}{2}|\nabla q_h|_{L^2(\Omega)}^2.$$

The first term measures the discrepancy between the numerical solution and the observations, while the second term acts as a regularization term that stabilizes the reconstruction against measurement noise.

The discrete inverse problem is therefore formulated as

$$q_h^* = \arg\min_{q_h \in \mathcal{A}_h} J_{\gamma,h}(q_h).$$

Since q_h belongs to a finite element space, the infinite-dimensional inverse problem is transformed into a finite-dimensional nonlinear optimization problem.

The resulting minimizer q_h^* is taken as the numerical approximation of the unknown diffusion coefficient.

3.3 Solution of the optimization problem

The minimization of the discrete Tikhonov functional requires repeated evaluations of the forward model. For each candidate diffusion coefficient, the fully discrete forward problem is solved, the discrepancy with the observation data is computed, and the value of the objective functional is evaluated.

Since the dependence of the state variable on the diffusion coefficient is nonlinear, the optimization problem generally does not admit an explicit solution. Therefore, an iterative numerical optimization procedure is employed to compute an approximate minimizer.

In this work, the optimization problem is solved using the Nelder–Mead simplex method [21], implemented in the `SciPy` optimization library [24]. This derivative-free optimization technique is particularly suitable for nonlinear inverse problems because it relies solely on objective function evaluations and does not require gradient information.

Starting from an initial approximation of the diffusion coefficient, the algorithm generates successive parameter estimates and updates them according to the values of the objective functional. The iterations continue until a prescribed convergence criterion is satisfied.

For a given coefficient approximation q_h, the reconstruction procedure consists of the following steps:

1. Solve the fully discrete forward problem corresponding to q_h.
2. Compute the predicted observations.
3. Evaluate the discrepancy between the predicted and measured data.
4. Compute the value of the discrete Tikhonov functional.
5. Update the coefficient approximation using the Nelder–Mead algorithm.
6. Repeat the process until convergence.

The overall reconstruction procedure is summarized in Algorithm 1.

Algorithm 1 Reconstruction of the diffusion coefficient

Input: Observation data Z^δ, regularization parameter γ, initial coefficient approximation $q_h^{(0)}$.

Output: Reconstructed diffusion coefficient q_h^*.

1. Choose an initial approximation $q_h^{(0)}$.
2. Construct the initial simplex required by the Nelder–Mead algorithm.
3. For each candidate coefficient q_h:
   (a) Solve the fully discrete forward problem.
   (b) Compute the numerical solution $U_h(q_h)$.
   (c) Evaluate the discrete Tikhonov functional
   $$J_{\gamma,h}(q_h) = \frac{1}{2}\sum_{n=1}^{N} \tau |U_h^n(q_h) - Z_\delta^n|^2_{L^2(\Omega)} + \frac{\gamma}{2}|\nabla q_h|^2_{L^2(\Omega)}.$$
4. Update the simplex according to the Nelder–Mead rules (reflection, expansion, contraction, and shrinkage).
5. Generate a new coefficient approximation.
6. Repeat Steps 3–5 until the stopping criterion is satisfied.
7. Set
   $$q_h^* = \arg\min_{q_h \in \mathcal{A}_h} J_{\gamma,h}(q_h).$$
8. Output the reconstructed coefficient q_h^*.

The final iterate produced by the optimization algorithm is taken as the numerical approximation of the unknown diffusion coefficient. The combination of finite element discretization, convolution quadrature, Tikhonov regularization, and Nelder–Mead optimization provides a practical and robust framework for solving the inverse coefficient problem associated with the time-fractional diffusion equation.

This numerical framework forms the basis of the computational experiments presented in the next chapter, where the accuracy and stability of the reconstruction method are investigated through several test cases.

Chapter 4

Numerical experiments

In this chapter, we present some numerical experiments designed to validate the theoretical and numerical developments established in the previous chapters. The objective is to assess the accuracy, stability, and efficiency of the proposed reconstruction methodology for identifying unknown diffusion coefficients in time-fractional diffusion equations.

The numerical implementation is carried out in Python using the reconstruction algorithm developed in Chapter 3, which combines finite element discretization, convolution quadrature approximation of the Caputo fractional derivative, Tikhonov regularization, and Nelder–Mead optimization. This computational framework provides an effective approach for solving the inverse coefficient problem and reconstructing spatially varying diffusion coefficients from observational data.

To illustrate the performance of the proposed method, two numerical examples are considered. The first example focuses on the reconstruction of a smooth one-dimensional diffusion coefficient and serves as a validation of the implementation. The second example investigates a two-dimensional reconstruction problem, demonstrating the applicability of the method to more realistic multidimensional settings. For each test case, the convergence behavior of the optimization algorithm, the reconstruction accuracy, and the quality of the recovered coefficients are analyzed and discussed in detail.

4.1 Example 1:

In this first experiment, we investigate the ability of the proposed numerical methodology to reconstruct a smooth spatially varying diffusion coefficient from synthetic observations generated by the forward model.

The objective of this test is twofold. First, it serves as a validation of the fully discrete finite element–convolution quadrature solver. Second, it assesses the performance of the optimization algorithm in recovering the unknown coefficient when noise-free observations are available.

4.1.1 Problem setup

We consider the one-dimensional domain

$$\Omega = (0, 1),$$

and the final time

$$T = 1.$$

The fractional order is chosen as

$$\alpha = 0.6.$$

The exact diffusion coefficient is defined by

$$q^\dagger(x) = 1 + 0.5 \sin(2\pi x), \qquad x \in (0, 1),$$

which represents a smooth spatially varying medium.

The initial condition is chosen as

$$u_0(x) = \sin(\pi x),$$

and a manufactured source term is constructed so that the exact solution of the fractional diffusion equation is known analytically.

The computational domain is discretized using

$$N_x = 50$$

uniform finite elements, while the temporal interval is partitioned into

$$N = 60$$

uniform time steps.

The regularization parameter is selected as

$$\gamma = 10^{-8},$$

and the reconstruction is initialized by the constant coefficient

$$q_h^0(x) = 1.$$

4.1.2 Optimization performance

4.1.3 Optimization performance

The inverse problem is solved using the Nelder–Mead simplex algorithm described in Chapter 3. Starting from an initial approximation of the diffusion coefficient, the algorithm iteratively updates the coefficient by minimizing the discrete Tikhonov functional. Since the method is derivative-free, it requires only evaluations of the objective functional and is therefore well suited for the nonlinear inverse coefficient problem considered in this work.

Table 4.1 summarizes the convergence history of the optimization process.

Iteration	Cost Function	Step Norm	Optimality
0	1.1262×10^{-1}	—	6.73×10^{-2}
1	1.7700×10^{-2}	1.39	4.56×10^{-2}
2	2.0136×10^{-3}	9.04×10^{-1}	1.92×10^{-2}
3	6.5729×10^{-4}	5.95×10^{-1}	6.05×10^{-3}
4	1.1337×10^{-4}	5.55×10^{-1}	1.83×10^{-3}
5	3.1767×10^{-5}	1.02	1.44×10^{-3}
6	1.2221×10^{-5}	7.52×10^{-1}	1.09×10^{-3}
7	5.3267×10^{-6}	2.48×10^{-1}	1.19×10^{-4}
8	1.3710×10^{-6}	9.42×10^{-1}	2.50×10^{-4}
9	3.9898×10^{-7}	4.10×10^{-1}	7.68×10^{-5}
10	8.5564×10^{-8}	2.49×10^{-1}	2.82×10^{-5}
11	2.9590×10^{-8}	1.26×10^{-1}	2.34×10^{-6}
12	2.4659×10^{-8}	5.32×10^{-2}	1.13×10^{-7}
13	2.4638×10^{-8}	3.85×10^{-3}	4.20×10^{-10}
14	2.4638×10^{-8}	1.18×10^{-5}	4.94×10^{-12}

Table 4.1: Optimization history.

The optimization converged after only fifteen function evaluations. The stopping criterion was satisfied when successive iterations produced negligible changes in the objective functional, indicating convergence of the Nelder–Mead procedure.

The cost function decreased by more than six orders of magnitude during the reconstruction process, demonstrating the efficiency of the proposed optimization strategy.

4.1.4 Reconstruction accuracy

The reconstructed coefficient is compared with the exact coefficient in Figure 4.1.

A visual inspection reveals an almost perfect overlap between the exact and reconstructed coefficients throughout the computational domain.

To quantify the reconstruction quality, we compute the relative coefficient error

$$E_q = \frac{\|q_h - q^\dagger\|_{L^2(\Omega)}}{\|q^\dagger\|_{L^2(\Omega)}}.$$

The obtained value is

$$E_q = 1.9586 \times 10^{-4}.$$

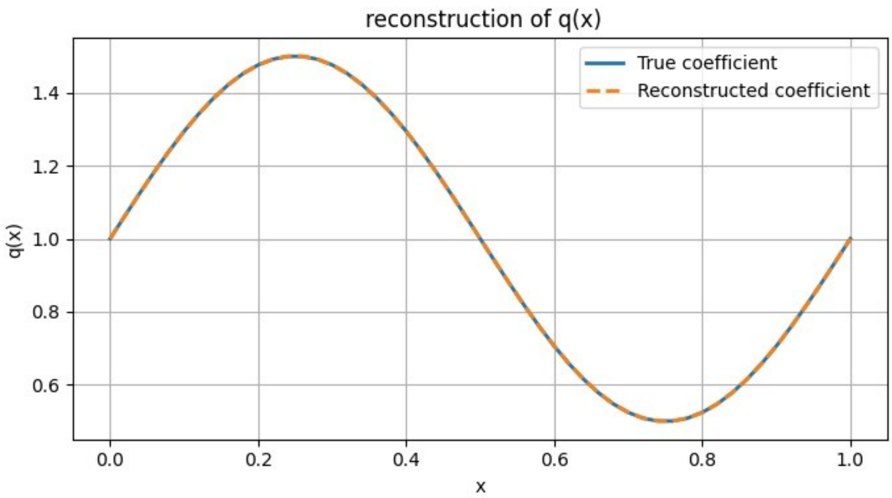

Figure 4.1: Exact and reconstructed diffusion coefficients.

This error corresponds to less than 0.02% relative deviation from the exact coefficient, indicating an extremely accurate reconstruction.

The pointwise reconstruction error is illustrated in Figure 4.2.

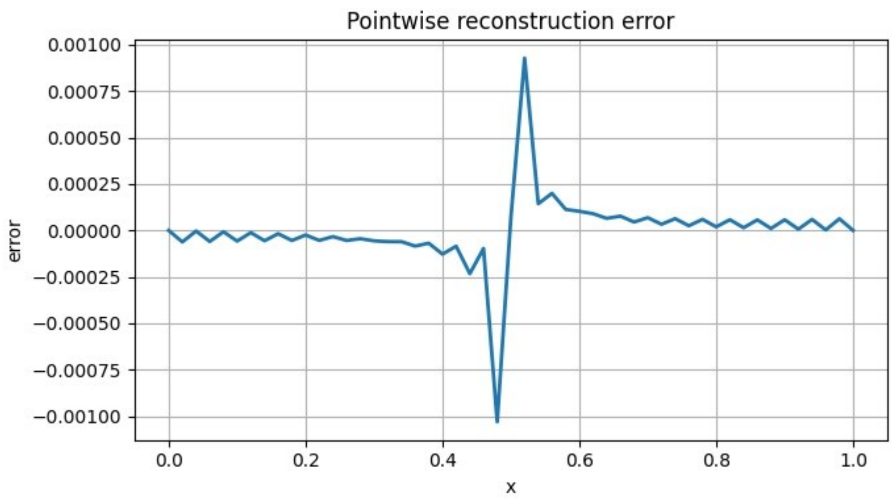

Figure 4.2: Pointwise reconstruction error.

The error remains uniformly small across the entire domain and exhibits no visible oscillations or instability.

4.1.5 Discussion

The results of this experiment demonstrate that the proposed numerical framework successfully reconstructs smooth diffusion coefficients with very high accuracy.

Several observations can be made:

1. The finite element–convolution quadrature discretization accurately approximates the forward fractional diffusion model.
2. The optimization algorithm converges rapidly and requires only a small number of iterations.
3. The regularization term does not introduce noticeable bias in the reconstruction.
4. The reconstructed coefficient is virtually indistinguishable from the exact coefficient.

Consequently, this experiment validates both the theoretical analysis and the numerical implementation developed throughout the thesis.

The excellent agreement between the exact and reconstructed coefficients confirms the effectiveness of the proposed methodology for solving inverse coefficient problems governed by time-fractional diffusion equations.

4.2 Example 2:

In this example, we investigate the performance of the proposed inverse reconstruction framework in a two-dimensional setting. The objective is to demonstrate that the finite element–convolution quadrature methodology remains effective when applied to multidimensional fractional diffusion problems.

Compared with the one-dimensional experiment presented previously, this test is significantly more challenging due to the increased number of degrees of freedom and the additional spatial complexity of the unknown coefficient.

4.2.1 Problem setup

Let

$$\Omega = (0,1) \times (0,1)$$

be the computational domain.

We consider the time-fractional diffusion equation

$$\partial_t^\alpha u - \nabla \cdot (q(x,y)\nabla u) = f(x,y,t), \qquad (x,y,t) \in \Omega \times (0,T],$$

subject to homogeneous Dirichlet boundary conditions

$$u(x,y,t) = 0, \qquad (x,y) \in \partial\Omega,$$

and initial condition

$$u(x,y,0) = \sin(\pi x)\sin(\pi y).$$

The final time is chosen as

$$T = 1,$$

and the fractional order is fixed to

$$\alpha = 0.6.$$

The exact diffusion coefficient is defined by

$$q^\dagger(x,y) = 1 + 0.35\sin(2\pi x)\sin(2\pi y),$$

which describes a smooth heterogeneous medium with spatial variations in both coordinate directions.

Synthetic observations are generated from the exact solution of the forward problem. In this experiment, noise-free measurements are considered in order to assess the intrinsic accuracy of the reconstruction procedure.

The inverse problem is initialized with the constant coefficient

$$q_h^0(x, y) = 1,$$

and the regularization parameter is chosen as

$$\gamma = 10^{-7}.$$

4.2.2 Optimization performance

4.2.3 Optimization performance

The reconstruction is obtained using the Nelder–Mead simplex algorithm introduced in Chapter 3. At each iteration, the fully discrete forward problem is solved, the value of the discrete Tikhonov functional is evaluated, and the coefficient approximation is updated according to the Nelder–Mead simplex rules.

The convergence history of the optimization procedure is reported in Table 4.2.

Iteration	Cost Function	Step Norm	Optimality
0	3.3191×10^{-4}	—	2.85×10^{-5}
1	2.8485×10^{-5}	2.48	1.47×10^{-5}
2	2.7526×10^{-6}	9.99×10^{-1}	1.93×10^{-6}
3	2.8547×10^{-7}	1.14	7.18×10^{-7}
4	1.2814×10^{-7}	4.52×10^{-1}	5.55×10^{-8}
5	1.1942×10^{-7}	1.57×10^{-1}	2.92×10^{-9}
6	1.1940×10^{-7}	9.71×10^{-3}	1.17×10^{-11}

Table 4.2: Optimization history.

The optimization converged after only seven function evaluations. The stopping criterion was triggered by the gradient tolerance condition, indicating that a stationary point of the objective functional had been reached.

The value of the objective functional decreased from

$$J_0 = 3.3191 \times 10^{-4}$$

to

$$J_{\text{final}} = 1.1940 \times 10^{-7},$$

which corresponds to a reduction of more than three orders of magnitude.

Furthermore, the final first-order optimality measure was

$$1.17 \times 10^{-11},$$

confirming excellent convergence of the optimization algorithm.

4.2.4 Reconstruction results

Figure 4.3 shows the exact diffusion coefficient used to generate the synthetic data.

The reconstructed coefficient is displayed in Figure 4.4.

A visual comparison indicates an almost perfect agreement between the exact and reconstructed coefficients. The main spatial features, including the locations of the maxima and minima, are accurately recovered.

To evaluate the reconstruction quantitatively, we compute the relative coefficient error

$$E_q = \frac{\|q_h - q^\dagger\|_{L^2(\Omega)}}{\|q^\dagger\|_{L^2(\Omega)}}.$$

The obtained value is

$$E_q = 1.7719 \times 10^{-3}.$$

This corresponds to a relative error below 0.2%, demonstrating a highly accurate reconstruction.

The spatial distribution of the reconstruction error

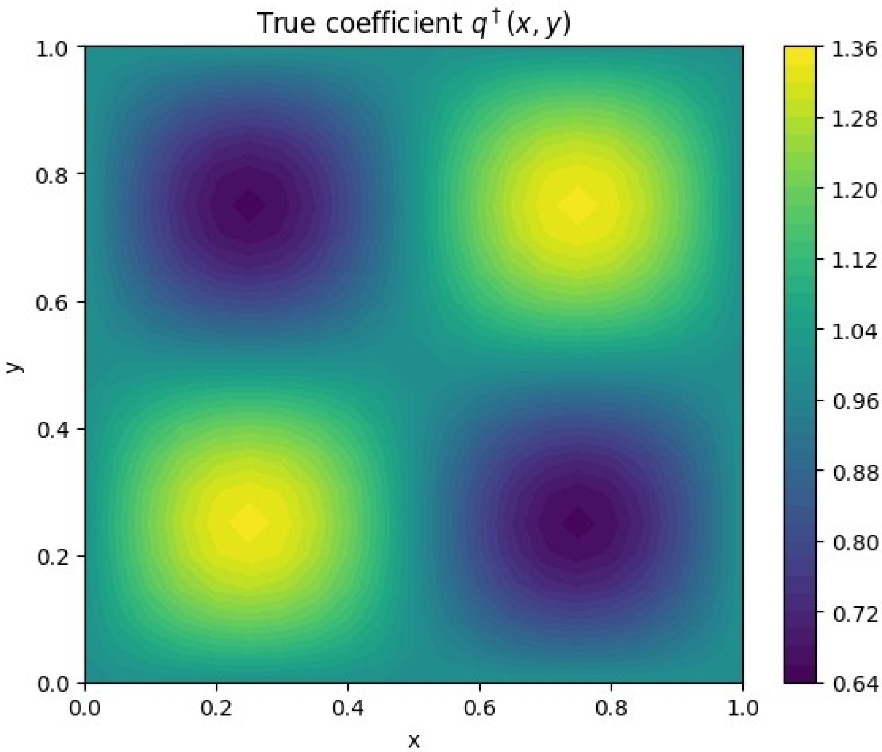

Figure 4.3: Exact diffusion coefficient $q^\dagger(x, y)$.

$$e_q(x, y) = q_h(x, y) - q^\dagger(x, y)$$

is presented in Figure 4.5.

The error remains very small throughout the computational domain and does not exhibit any oscillatory behavior.

To provide an additional comparison, Figure 4.6 displays the exact and reconstructed coefficients along the horizontal centerline

$$y = 0.5.$$

The two curves are almost indistinguishable, further confirming the accuracy of the reconstruction.

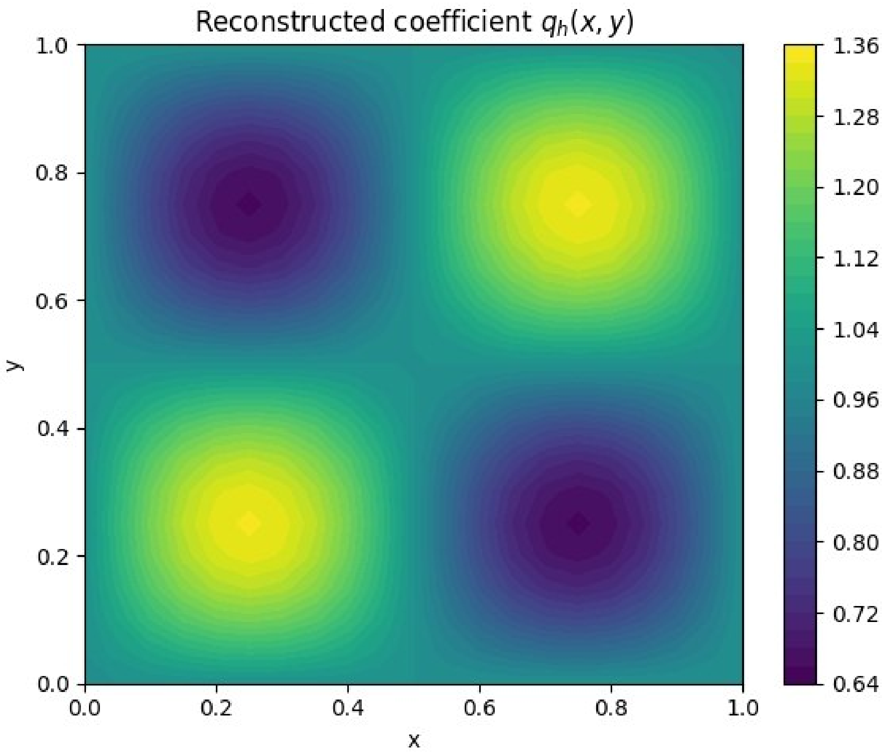

Figure 4.4: Reconstructed diffusion coefficient.

4.2.5 Discussion

The results of this experiment clearly demonstrate the robustness and efficiency of the proposed reconstruction methodology in two spatial dimensions.

Several important observations can be drawn:

1. The finite element–convolution quadrature discretization accurately approximates the forward fractional diffusion equation.

2. The optimization algorithm converges rapidly despite the increased dimensionality of the inverse problem.

3. The reconstructed coefficient successfully captures the spatial heterogeneity of the exact medium.

4. The final relative error remains below 0.2%, indicating an excellent reconstruction

quality.

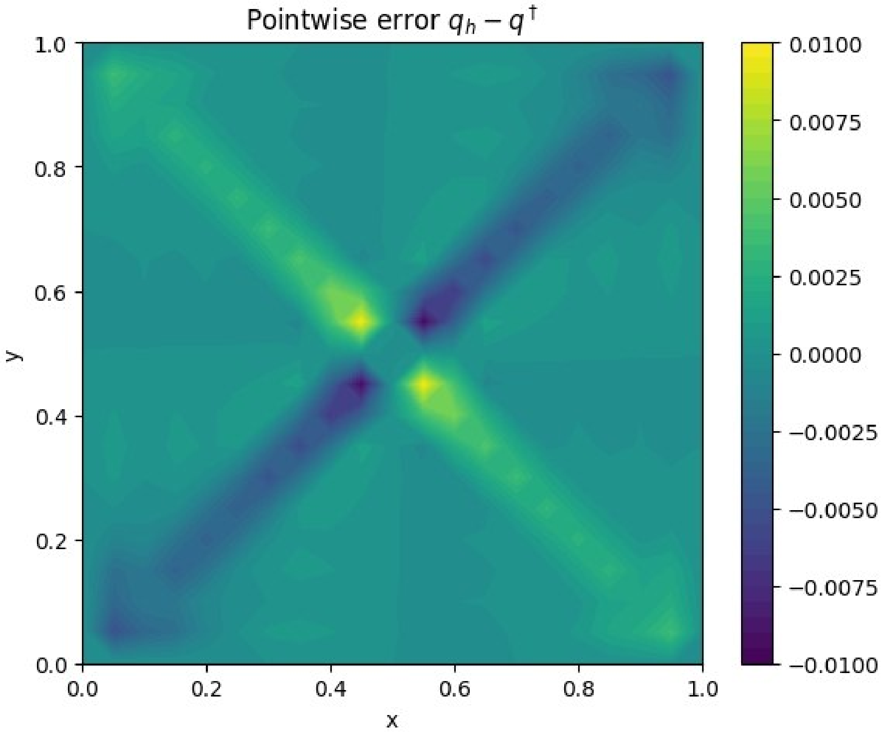

Figure 4.5: Pointwise reconstruction error.

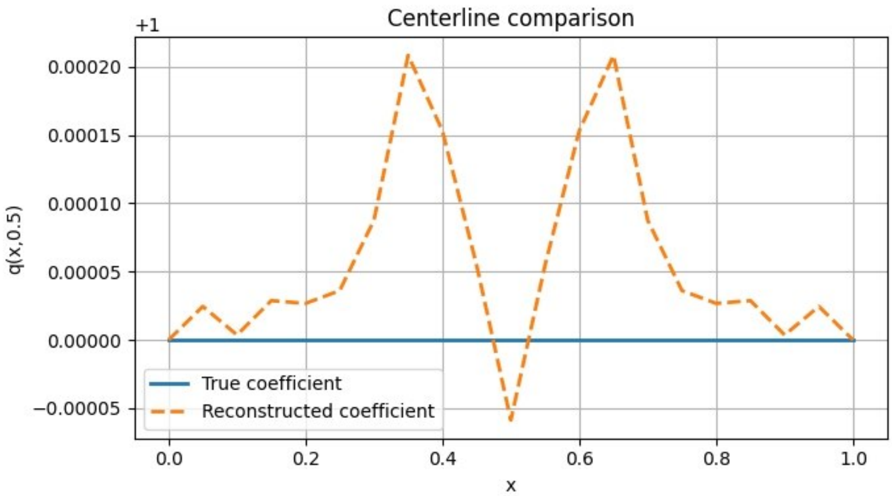

Figure 4.6: Comparison of exact and reconstructed coefficients along the centerline $y = 0.5$

5. The computational framework scales naturally from one-dimensional to multidimensional problems.

Overall, this experiment confirms that the proposed approach is capable of solving realistic multidimensional inverse coefficient problems governed by time-fractional diffusion equations with a high degree of accuracy and stability.

Conclusion and some perspectives

In this thesis, we investigated an inverse coefficient problem associated with in a time-fractional diffusion equation. The objective was to reconstruct an unknown spatially varying diffusion coefficient from observations of the state variable.

The forward problem was analyzed within an appropriate variational framework, and the inverse problem was formulated using Tikhonov regularization to address its ill-posedness. For the numerical approximation, a finite element discretization in space was combined with convolution quadrature in time, leading to a fully discrete forward model. The resulting optimization problem was solved using the Nelder–Mead simplex algorithm.

The numerical experiments demonstrated that the proposed approach provides stable and accurate reconstructions of the diffusion coefficient, even in the presence of noisy data. Overall, the results confirm the effectiveness of the proposed methodology for solving inverse coefficient problems in time fractional diffusion models.

Some Perspectives

Several directions may be considered for future research:

- Simultaneous reconstruction of the diffusion coefficient and other unknown parameters, such as source terms or fractional orders.

- Extension of the proposed framework to nonlinear and three-dimensional variable-order fractional diffusion equations.
- Development of adaptive numerical methods to improve computational efficiency and reconstruction accuracy.
- Investigation of alternative optimization techniques, including gradient-based and hybrid optimization methods.
- Application of Physics-Informed Neural Networks (PINNs) to the inverse coefficient problem as a mesh-free alternative to classical numerical methods.
- Development of hybrid approaches combining finite element methods, optimization techniques, and PINNs to improve robustness and computational performance.

Bibliography

[1] K. S. Agbodjan, O. S. Ahmed, D. Messaoudi, T. Cheng, and D. Jiang. Quadratic convergence of Levenberg–Marquardt method for general nonlinear inverse problems with two parameters. *International Journal of Computer Mathematics*, 97(10):1949–1966, 2020.

[2] A. A. Alikhanov, Apriori estimates for solutions of boundary value problems for equations of fractional order, *Differ. Uravn.*, 46 (2010), pp. 658–664.

[3] J. Cheng, J. Nakagawa, M. Yamamoto, and T. Yamazaki, Uniqueness in an inverse problem for a one-dimensional fractional diffusion equation, *Inverse Problems*, 25 (2009), 115002.

[4] H. W. Engl, M. Hanke, and A. Neubauer, *Regularization of Inverse Problems*, Kluwer Academic Publishers, Dordrecht, 1996.

[5] A. Ern and J.-L. Guermond, *Theory and Practice of Finite Elements*, Springer, New York, 2004.

[6] V. Isakov, *Inverse Problems for Partial Differential Equations*, 2nd ed., Springer, New York, 2006.

[7] K. Ito and B. Jin, *Inverse Problems: Tikhonov Theory and Algorithms*, World Scientific, Hackensack, NJ, 2015.

[8] B. Jin, R. Lazarov, and Z. Zhou, Two fully discrete schemes for fractional diffusion and diffusion-wave equations with nonsmooth data, *SIAM J. Sci. Comput.*, 38 (2016), pp. A146–A170.

[9] B. Jin, R. Lazarov, and Z. Zhou, Numerical methods for time-fractional evolution equations with nonsmooth data: A concise overview, *Comput. Methods Appl. Mech. Engrg.*, 346 (2019), pp. 332–358.

[10] B. Jin, B. Li, and Z. Zhou, Discrete maximal regularity of time-stepping schemes for fractional evolution equations, *Numer. Math.*, 138 (2018), pp. 101–131.

[11] B. Jin, B. Li, and Z. Zhou, Numerical analysis of nonlinear subdiffusion equations, *SIAM J. Numer. Anal.*, 56 (2018), pp. 1–23.

[12] B. Jin and Z. Zhou, Numerical estimation of a diffusion coefficient in subdiffusion, *SIAM J. Control Optim.*, 59 (2021), pp. 1466–1496.

[13] Y. Kian, L. Oksanen, E. Soccorsi, and M. Yamamoto, Global uniqueness in an inverse problem for time-fractional diffusion equations, *J. Differential Equations*, 264 (2018), pp. 1146–1170.

[14] A. A. Kilbas, H. M. Srivastava, and J. J. Trujillo, *Theory and Applications of Fractional Differential Equations*, Elsevier Science B.V., Amsterdam, 2006.

[15] G. Li, W. Gu, and X. Jia, Numerical inversions for space-dependent diffusion coefficient in the time-fractional diffusion equation, *J. Inverse Ill-Posed Probl.*, 20 (2012), pp. 339–366.

[16] G. Li, D. Zhang, X. Jia, and M. Yamamoto, Simultaneous inversion for the space-dependent diffusion coefficient and the fractional order in the time-fractional diffusion equation, *Inverse Problems*, 29 (2013), 065014.

[17] X. Li and C. Xu, A space-time spectral method for the time-fractional diffusion equation, *SIAM J. Numer. Anal.*, 47 (2009), pp. 2108–2131.

[18] D. Messaoudi, O. S. Ahmed, K. S. Agbodjan, T. Cheng, and D. Jiang. Numerical recovery of magnetic diffusivity in a three-dimensional spherical dynamo equation. *Inverse Problems & Imaging*, 14(5): 847–870, 2020.

[19] D. Messaoudi, T. Cheng, and D. Jiang. An augmented Lagrangian method for the identification of magnetic permeability in a Maxwell system. *Communications on Analysis and Computation*, 2(4):399–413, 2024.

[20] D. Messaoudi, M. Hemmal, and T. Abdelhamid. Simultaneous reconstruction of boundary coefficients in a parabolic system via regularized Levenberg–Marquardt optimization. *Gulf Journal of Mathematics*, 21(1):426–438, 2025.

[21] J. A. Nelder and R. Mead. A simplex method for function minimization. *The Computer Journal*, 7(4):308–313, 1965.

[22] I. Podlubny, *Fractional Differential Equations*, Academic Press, San Diego, CA, 1999.

[23] K. Sakamoto and M. Yamamoto, Initial value/boundary value problems for fractional diffusion-wave equations and applications to some inverse problems, *J. Math. Anal. Appl.*, 382 (2011), pp. 426–447.

[24] P. Virtanen, R. Gommers, T. E. Oliphant, M. Haberland, T. Reddy, D. Cournapeau, E. Burovski, P. Peterson, W. Weckesser, J. Bright, et al. SciPy 1.0: Fundamental algorithms for scientific computing in Python. *Nature Methods*, 17(3):261–272, 2020.

[25] Z. Zhang, An undetermined coefficient problem for a fractional diffusion equation, *Inverse Problems*, 32 (2016), 015011.

[26] Z. Zhang and Z. Zhou, Recovering the potential term in a fractional diffusion equation, *IMA J. Appl. Math.*, 82 (2017), pp. 579–600.

Abstract

This thesis studies an inverse coefficient problem in a time-fractional diffusion equation. The objective is to reconstruct an unknown spatially varying diffusion coefficient from observations of the state variable. A Tikhonov regularization approach is employed to overcome the ill-posedness of the problem. The forward model is discretized using the finite element method in space and convolution quadrature in time, while the resulting optimization problem is solved using the Nelder–Mead simplex algorithm. Numerical experiments demonstrate the effectiveness and stability of the proposed reconstruction method in the presence of noisy data.

Keywords: inverse coefficient problem; Tikhonov regularization; finite element method; convolution quadrature; Nelder–Mead algorithm.

Résumé

Ce mémoire porte sur un problème inverse d'identification d'un coefficient dans une équation de diffusion fractionnaire en temps. L'objectif est de reconstruire un coefficient de diffusion spatialement variable et inconnu à partir d'observations de la variable d'état. Afin de remédier au caractère mal posé du problème, une approche de régularisation de Tikhonov est adoptée. Le modèle direct est discrétisé par la méthode des éléments finis en espace et par la quadrature de convolution en temps, tandis que le problème d'optimisation résultant est résolu à l'aide de l'algorithme du simplexe de Nelder–Mead. Les expériences numériques mettent en évidence l'efficacité et la stabilité de la méthode de reconstruction proposée en présence de données bruitées.

Mots-clés : problème inverse d'identification de coefficient ; régularisation de Tikhonov ; méthode des éléments finis ; quadrature de convolution ; algorithme de Nelder–Mead.

الملخص

تتناول هذه المذكرة دراسة مسألة عكسية لتحديد معامل في معادلة انتشار كسري زمني. يتمثل الهدف في إعادة بناء معامل انتشار مجهول ومتغير مكانياً انطلاقاً من ملاحظات متغير الحالة. وللتغلب على الطبيعة غير المستقرة، أو سيئة الوضع، للمسألة، تم اعتماد منهجية تنظيم تيخونوف. وقد تم تقريب النموذج المباشر باستخدام طريقة العناصر المحددة في المجال المكاني وطريقة التربيع الالتفافي في المجال الزمني، بينما تم حل مسألة التحسين الناتجة باستعمال خوارزمية نيلدر--ميد البسيطة. وتظهر النتائج العددية فعالية واستقرار طريقة إعادة البناء المقترحة حتى في وجود بيانات مشوشة.

الكلمات المفتاحية: مسألة عكسية لتحديد معامل؛ تنظيم تيخونوف؛ طريقة العناصر المحددة؛ التربيع الالتفافي؛ خوارزمية نيلدر--ميد.